Tang, T. Y. D., Cecchi, D., Fracasso, G., Accardi, D., Coutable-Pennarun, A., Mansy, S. S., Perriman, A. W., Anderson, J. L. R., & Mann, S. (2018). Gene-Mediated Chemical Communication in Synthetic Protocell Communities. *ACS Synthetic Biology*, *7*(2), 339-346. https://doi.org/10.1021/acssynbio.7b00306

Gene-mediated chemical communication in synthetic protocell communities

T-Y. Dora Tang[1,6*], Dario C. Cecchi[2], Giorgio Fracasso[1], Davide Accardi[1], Angelique Coutable[3,6], Sheref S. Mansy[2], Adam W. Perriman[4,6], J. L. Ross Anderson[3,6], Stephen Mann[5,6*]

[1]Max Planck Institute of Molecular Cell Biology and Genetics, 01307 Dresden, Germany; [2]CIBIO, University of Trento, via Sommarive 9, 38123 Povo, Italy; [3]School of Biochemistry and [4] School of Cellular and Molecular Medicine, University of Bristol, Bristol BS8 1TD, United Kingdom; [5]Centre for Protolife Research, School of Chemistry, University of Bristol, Bristol BS8 1TS, United Kingdom; [6]BrisSynBio Synthetic Biology Research Centre, Life Sciences Building, University of Bristol, Tyndall Avenue, Bristol BS8 1TQ, UK

Abstract: A gene-directed chemical communication pathway between synthetic protocell signaling transmitters (lipid vesicles) and receivers (proteinosomes) was designed, built and tested using a bottom-up modular approach comprising small molecule transcriptional control, cell-free gene expression, porin-directed efflux, substrate signaling, and enzyme cascade-mediated processing.

Keywords: communication, cell-free expression, lipid vesicles, proteinosomes, genetic switches, enzyme cascade, α-hemolysin

The design of novel artificial cells, engineering of new genetic circuits and switches, and optimization of cell-free gene expression systems are providing invaluable technologies in synthetic biology. Advances in these areas have inspired the design and construction of a range of synthetic protocells, including membrane-bound compartments such as lipid vesicles[1,2], proteinosomes[3,4], polymersomes[5,6], colloidosomes[7] and water-in-oil emulsions[8,9], as well as membrane free coacervate micro-droplets[10]. These micro-compartmentalized systems are capable of encapsulating and supporting a range of complex biochemical processes such as enzyme cascade reactions[4,5,11,12], cell-free gene expression[13-16], replication[17,18], transcriptionally-derived oscillatory reactions[19], growth and division[20], and protocell fusion[21]. In conjunction, new rationally designed genetic modules based on the integration and exchange of custom-made gene circuits have been incorporated into cell-free systems[22,23] and minimal cells[2] to increase the level of transcriptional and translational control.

Whilst the majority of the current investigations have focused on the construction and functionalization of discrete protocellular compartments, routes towards chemical signalling pathways between living cells and protocells have been proposed [24,25] and a number of recent studies have investigated this possibility. For example, lipid vesicles have been exploited as unidirectional and bidirectional translators and communicators to bacterial cells via carbohydrate or riboswitch dependent mechanisms[26-28]. In other studies, aligned water-in-oil droplets containing an encapsulated cell-free gene expression system or bacteria have been shown to act as a transmitter and receiver system of a small molecule transciption inducer produced in situ[29].

The above studies demonstrate the potential and utility of synthetic protocells as modules for building consortia with living organisms based on gene-directed, multi-enzyme networks for signalling, communication and information processing. In contrast, the possibility of enacting similar processes in mixed communities comprising only synthetic protocells remains relatively unexplored. Recently, collective interactions in synthetic protocell communities have been exploited for rudimentary predatory behaviour[30], artificial phagocytosis[31] and chemical communication[32]. For the most part, these systems involve sequential enzymatic interactions within binary populations of synthetic protocells, or a gene-mediated pathway between one type of protocell[33] but to date there is no demonstration of gene-directed chemical communication between two different populations of protocells.

In this paper we describe the design, assembly and testing of a gene-mediated chemical communication pathway between two populations of synthetic protocells using a modular bottom-up approach (Fig. 1). The signaling pathway is uni-directional and based on lipid vesicle transmitters and proteinosome receivers. The vesicles contain an encapsulated cell-free expression system (PURExpress); a DNA plasmid programmed with a chemically inducible repression switch (EsaR) and a gene coding for α-hemolysin; and a signaling molecule (glucose). In contrast, the proteinosomes consist of a cross-linked enzymatically active glucose oxidase (GOx)-poly(N-isopropylacrylamide) (PNIPAAM) membrane and encapsulated horseradish peroxidase (HRP). We show that addition of a lipid membrane permeable small molecule transcription inducer N-(3-Oxohexanoyl)-L-homoserine lactone (3OC6HSL) triggers intravesicular α-hemolysin expression and membrane pore formation, which in turn faciliates the release of glucose. Consequently, oxidation of glucose on the proteinosome membrane produces hydrogen peroxide, which converts Amplex red to a fluorescent output by reaction with encapsulated HRP. To the best of our knowledge, this is the first example of gene-directed chemical communication in a binary synthetic protocell community, and provides a step towards designing and constructing signaling pathways in mixed populations of artificial cell-like constructs.

Results and discussion:

Lipid vesicles containing a DNA plasmid, cell-free gene expression system and molecular substrates were prepared according to established procedures (Materials and Methods, and SI Methods). The plasmids consisted of a T7 promoter coupled to an *esaO* operator and gene for a membrane porin α-hemolysin (DC055a) or GFP-tagged α-hemolysin (DC061a), and a T7 promoter coupled to a gene coding for an *esaO*-binding repressor protein (EsaR) that was responsive to 3OC6HSL. To ascertain the activity of the EsaR repressor switch, we performed test experiments in bulk solutions (14 μL; no vesicles) containing the cell-free transcription/translation system and plasmid pET21b/*esao*/RFP expressing red fluorescent protein (RFP) (DC054a). Fluorescence spectra recorded at λ_{max} = 595 nm indicated that protein synthesis and folding occurred within 3 h at 37°C both in the absence and presence of the 3OC6HSL transcription inducer at plasmid and inducer concentrations of up to 1000 ng and 10 μM, respectively (Fig. S1). The difference between the level of leaky (non-induced) expression and induced expression was maximized by increasing the plasmid concentration to an optimal value of 800 ng/14 μL at a constant 3OC6HSL concentration of 10 μM (Fig. 2a), indicating that the effectiveness of the EsaR repressor switch was dependent on the inducer to plasmid ratio. Under optimal conditions, there was a 30% difference between induced and non-induced RFP expression, indicating that the EsaR repressor was functionally effective and compatible with the PURExpress system.

Based on these results, we tested whether 3OC6HSL-induced transcription and cell-free gene expression could be triggered within the aqueous lumen of multilamellar vesicles by passive influx of 3OC6HSL across the phospholipid bilayer. Moreover, as the vesicle to proteinosome communication pathway necessitated the expression and membrane insertion of a porin to release the glucose signaling molecules, we replaced the RFP gene with a gene coded for GFP-tagged α-hemolysin (pET21b/*esaO*/α-hemolysin-GFP (DC061a)), which was encapsulated along with the PURExpress system within vesicles prepared from a 1:2 mixture of POPC and cholesterol. The vesicles were imaged using fluorescence confocal microscopy in the presence or absence of 3OC6HSL after incubation at 37°C for 3 h. Although green fluorescence associated with GFP-tagged α-hemolysin expression was recorded in both cases, 40% of the vesicles exposed to the transcription inducer exhibited fluorescence intensities greater than the average fluorescence measured for vesicles displaying non-

induced (leaky) GFP expression (Fig S2). Closer inspection of the vesicles undergoing spatially confined gene-mediated protein synthesis showed regions of localized green fluorescence close to the inner leaflet of the membrane and within the vesicle lumen (Fig 2b). High temporal and spatial resolution confocal microscopy imaging of the localized fluorescence revealed a bimodal distribution of diffusion coefficients consisting of smaller (slower) (2×10^{-2} μm s^{-1} +/- 0.9×10^{-2} μm s^{-1}) or larger (faster) (2.0×10^{-1} μm s^{-1} +/- $1.1\ 10^{-1}$ μm s^{-1}) values associated with fluorescent entities imaged close to the membrane or within the lumen of the vesicles, respectively (Fig. S3). The smaller diffusion coefficients were comparable to values previously determined for membrane proteins within lipid membranes[34,35], strongly suggesting that the expressed GFP-tagged α-hemolysin was inserted into the bilayer membrane of the lipid vesicles.

Given the above observations, the effectiveness of expressed α-hemolysin to increase the permeability of the multilamellar vesicle membrane and hence accelerate the efflux rate of encapsulated small molecules was tested. For this, calcein was encapsulated within the vesicles at a dye concentration (80 mM) high enough to curtail the fluorescence intensity by intermolecular quenching[36,37], and incubated the protocells in an aqueous solution of PURExpress and plasmid DNA - pET21b/*esaO*/α-hemolysin (DC055a) with or without the transcription inducer. In both cases, kinetic assays showed a lag period followed by an increase in fluorescence intensity associated with a decrease in encapsulated calcein concentration. In contrast, no lag time was observed when a solution of purified α-hemolysin was added directly to the calcein-containing vesicles (Fig. S4), consistent with the requirement for an induction period associated with gene expression of the porin. Significantly, the increase in membrane permeability observed in the gene-mediated system in the presence of 3OC6HSL was considerably higher (~ 350 % increase in calcein fluorescence) than in the absence of the inducer after 1 h and 50 mins (Fig 2c). In contrast, control experiments in which the DC061a plasmid was replaced with a control plasmid with a T7 promoter and gene encoding for the non-porin protein, calmodulin (PEXP5-NT/CALML3) showed only minimal leakage of calcein from the vesicles (Fig 2c). The results confirmed that folding and self-assembly of the expressed α-hemolysin was sufficiently robust to facilitate insertion of the porin into the lipid membrane, thereby providing a gene-mediated mechanism for triggered release of calcein from the vesicles.

Taken together, the above observations were consistent with passive diffusion of 3OC6HSL through the phospholipid membrane, and retention of a responsive EsaR repressor switch and functional transcriptional/translational machinery within the vesicles. Moreover, activation of the switch increased the effectiveness of membrane pore formation with respect to the release of a potential signaling molecule from the vesicles. To test whether gene-mediated release of a small molecule could be coupled the to a positive read-out signal, PURExpress, a plasmid pET21b/*esaO*/α-hemolysin (DC055a), and glucose were encapsulated within the lipid vesicles, and the protocells incubated at 37°C in a solution containing GOx, HRP and Amplex red with or without the 3OC6HSL transcription inducer. We reasoned that gene-mediated release of glucose via *in situ* insertion of the expressed porin would initiate an enzyme cascade reaction in the bulk solution to produce resorufin as the red fluorescent output. Fluorescence spectra confirmed that gene-mediated glucose signaling to the GOx/HRP enzyme cascade was operational over *ca.* 3 h, and that the production of resorufin as determined from the end point data was significantly increased in the presence of 10 μM 3OC6HSL (Fig. 2d and Fig. S5). Resorufin was also detected in control experiments undertaken on vesicles without the encapsulated plasmid (Fig 2d). We attributed this to background levels of released glucose associated with vesicle fusion and breakage, and non-specific (non-porin-mediated) diffusion across the lipid membrane.

Having designed, built and tested a vesicle-based protocell model capable of acting as a potential signaling transmitter, we sought to combine this functionality with a receiver protocell as a step towards gene-mediated chemical communication in a community of cell-like colloidal objects. As a model of a receiver protocell, we designed and constructed proteinosomes with spatially distributed biocatalysts capable of performing an enzyme cascade reaction (Fig. S6). Specifically, the enzymatically active proteinosomes consisted of a semi-permeable membrane of crosslinked GOx-PNIPAAm nanoconjugates enclosing an aqueous solution of encapsulated HRP[11]. An approximately constant number of vesicles containing encapsulated PURExpress, glucose, and plasmid DNA (DC055) were mixed at 37 °C with a buffered dispersion of the HRP-containing GOx/PNIPAAM proteinosomes to produce a binary population containing intact protocells (Fig. 3a). Amplex red and either 3OC6HSL or an equivalent volume of HEPES solution were added to the mixed population and resorufin production monitored over 15 h at 37 °C as a proxy for the gene-mediated transmission and delivery of a functional chemical signal (glucose) from the vesicles to the enzymatically active proteinosomes.

A fluorescent read-out was observed almost immediately after addition of Amplex red in the presence or absence of the transcription inducer and was sustained for *ca.* 90 min after which a threshold value was attained (Fig. 3b). Significantly, the production of resorufin in the proteinosomes was typically increased by addition of 10 μM 3OC6HSL to vesicles prepared in the presence of high plasmid concentrations (2000 ng) (Fig. 3b). However, there was marked variability in the response behavior as presented in the raw data (Fig. S7) that made it difficult to discern clearly between systems operating in the presence or absence of 3OC6HSL. To circumvent this problem, we undertook multiple experiments in parallel using a plate well reader loaded with at least five aliquots of a single batch of the vesicle/proteinosome reaction mixture, and fitted the data using a logistic model to obtain the stationary points (time values on each curve where the second derivative = 0) for both induced (X_1^+) and non-induced (X_1^-) communication (Fig. 3c). Non-systematic residuals to the logistic fit showed that the model was valid for making semi-quantitative comparisons between experiments (Fig. S8). For each batch of vesicles and proteinosomes, we determined the average percentage difference ($[X_1^+ - X_1^-]/X_1^- \times 100$] between the stationary points obtained in the presence or absence of 3OC6HSL at different plasmid concentrations. Compared to the percentage difference in resorufin concentration determined for vesicles prepared with 0 ng of plasmid (-15%), a progressive increase in the percentage difference of *ca*. + 0% and +20 % was observed for vesicles prepared at 1000 and 2000 ng of plasmid, respectively (Fig. 3d). This showed that progressively increasing the plasmid concentration led to increased discrimination between gene expression arising from a responsive EsaR repressor switch and background levels associated with leaky gene expression. The results also indicated that at increasing amounts of plasmid and under the activity of 3OC6HSL, production of resorufin was more sustained than in the absence of the transcription factor. Moreover, it seems feasible that at low levels of α-hemolysin expresssion, the amount of adventitious (non-porin-mediated) glucose release contributes considerably to the efflux profile such that the gene-directed pathway becomes progressively over-ridden. Interestingly, a negative percentage difference was determined in the absence of the plasmid, indicating that the background release of glucose giving rise to adventitious resorufin production was reduced in the presence of 3OC6HSL, possibly through interactions with the lipid membrane. A similar effect was observed for the non-specific leakage of calcein in the absence of porin expression (Fig. 2c).

In conclusion, we use a molecular modular approach to design, build and test two protocell models capable of transmitting or receiving a chemical signal as a step towards a gene-mediated communication pathway for remote triggering of enzyme activity in a binary community of synthetic

cell-like objects. We employ a small molecular transcription inducer to activate a repressor switch that initiates the cell-free gene expression of α-hemolysin in a population of vesicles. The porin facilitates the efflux of glucose, which signals to an enzyme cascade housed within the membrane and interior of a population of proteinosomes to generate a fluorescent read-out. Although our modular approach provided an opportunity to optimize each component and incrementally increase the complexity of the system, we encountered considerable noise when we increased the molecular complexity to the level of protocell-protocell interactions. The increased level of noise can be attributed to various factors that together increase the stochasticity of the transmitter/receiver system. In the case of the vesicles, incomplete sets of the PURExpress components and insufficient numbers of plasmids produced by low encapsulation efficiencies are likely to be major factors[38,33], along with variations in the background leakage of glucose due to different levels of adventitious vesicle breakage and fusion, and membrane (multilamellar) thickness. Moreover, the repression switch may be compromised particularly during the initial stages of transcription because of the lag time required for the repressor protein EsaR to be expressed in sufficient quantities; as a consequence, α-hemolysin expression could be unhindered and the 3OC6HSL inducer ineffective during this time period, resulting in variable levels of incipient pore formation and glucose release. Whilst most of the elevated noise probably arises from the transmission system, we cannot rule out compounding factors associated with variations in the enzyme activity of individual proteinosome receivers, especially if the amount of glucose released was in excess of the turnover rate. In particular, the GOx enzyme is cationized and cross-linked into the protein-polymer membrane and these processes introduce a degree of statistical variation in the activity of the enzyme population.

Future experiments will be focused at increasing the fidelity of the vesicle/proteinosome communication system. For example, it should be possible to reduce the stochasticity and potentially the noise by using microfluidic strategies to generate synthetic protocells with controlled volumes and internalized concentrations. Moreover, replacing glucose with a charged substrate such as glucose-6-phosphate should alleviate problems associated with non-specific diffusion through the vesicle membrane provided that an appropriate enzyme pathway can be re-designed into the proteinosomes. However, it seems unlikely that noise will be eliminated entirely from these systems due to the number of components that are required to build protocell-protocell communication pathways in communities of disparate cell-like objects. Indeed, if the presence of noise in gene expression is crucial to controlling key biological processes[39-42], then minimal systems based on rudimentary forms of protocell communication could provide useful models for investigating stochastic processes *in vitro*.

Methods

Preparation of protocells: *Lipid vesicles***:** Stock solutions of POPC (40 mg/mL) and cholesterol (in 10 mg/mL) were prepared in chloroform and then mixed in a round bottom flask to achieve a final molar ratio of 1:2 POPC : cholesterol. The solvent was completely removed using a rotavapor to produce a lipid film, which was rehydrated in 2 mL of nuclease-free water. The solution was subjected to freeze/thaw cycles in liquid nitrogen and then warm water until all the lipid had re-dissolved and a turbid solution was formed. The vesicles were extruded ten times with a 1 µm filter and then aliquoted into 100 µL portions, lyophilised, and then stored at -20°C until used for the experiments. *Proteinosomes***:** Aqueous dispersions of HRP-encapsulated GOx-PNIPAAm semi-permeable microcapsules were prepared by water droplet/oil interfacial assembly, membrane crosslinking, and phase transfer using methods described previously[12] (Supplementary Information). In brief, an

aqueous buffered (HEPES, pH 7.6) solution of GOx-PNIPAAM nanoconjugates (45 μL; 8 mg/mL) and HRP 15μL; 20 mg/mL) was mixed with ethyl-1-hexanol (1.5 mL) containing PEGylated bis(sulfosuccinimidyl)suberate) (protein-crosslinking agent; BS(PEG)9; Mw =708.71; 0.1 mM), and shaken vigorously by hand for at least 60 s to produce a water-in-oil emulsion. The emulsion was left in the dark for 2 days, after which the excess oil was removed and the crosslinked proteinosomes transferred into 70 % ethanol/water followed by dialysis against 70% ethanol/water (2 h), Milli-Q water (22 h), and then HEPES buffer (2 h). Aqueous dispersions of the proteinosomes were stored at 4°C.

Encapsulation of genetic machinery within lipid vesicles: Before encapsulation, PURExpress was prepared as directed by the manufacturer's instructions. A DNA plasmid (0.5-2 μg) consisting of a T7 promoter coupled to an *esaO* operator and gene for a membrane porin (α-hemolysin (DC055a, Mw = 3657331 Da) or GFP-tagged α-hemolysin (DC061a, Mw = 4152268.40 Da), and a T7 promoter coupled to a gene coding for a 3OC6HSL-responsive *esaO*-binding repressor protein (EsaR) was added to a PURExpress solution (final volume, 25 μL). Glucose (2.5 μL; 2.5 M) was also added in the signalling experiments. 25 μL of the PURE/plasmid/(glucose) mixture was then added to a 100 μL aliquot of the lyophilised POPC/cholesterol lipid vesicles, and vortexed to completely re-disperse the vesicles. The lipid vesicles were dialysed against HEPES buffer at 4°C for 2 h using a home-made dialysis membrane[43] to remove all non-encapsulated cell free expression components and glucose.

Determination of activity of EsaR switch: The activity of the EsaR repressor switch was tested in the absence of vesicles using aqueous solutions containing PURExpress and a plasmid DNA pET21b/*esaO*/RFP for red fluorescent protein (RFP; DC054a, Mw = 3680261.40 Da) expression. A range of plasmid concentrations (200 to 1000 ng in 14 μL (final volume) of PURExpress reaction mixture) was used. Either 10 μM of 3OC6CHSL or the equivalent aqueous volume of HEPES was added for each different plasmid concentration. The sample solution was incubated at 37°C for 3 hours, after which the fluorescence spectra associated with RFP expression (λ_{exc} 563 nm, λ_{emi} 582-700 nm) were recorded. The percentage difference between the peak maxima at 595 nm obtained for the 3OC6CHSL-induced and non-induced protocols was determined as a measure of EsaR activity.

Cell-free gene expression of GFP-tagged α-hemolysin within lipid vesicles: Lipid vesicles containing an encapsulated solution of PURExpress, pET21b/*esaO*/α-hemolysin-GFP (DC061a) were prepared as described above. Dialysed vesicles were incubated for 3 hours with gentle shaking at 37°C in the presence or absence of the small-molecule membrane-permeable inducer N-(3-Oxohexanoyl)-L-homoserine lactone (3OC6HSL) (Mw= 213.23 g mol^{-1}; 10 μM). Cell-free gene expression of GFP-tagged α-hemolysin within the vesicles was monitored by fluorescence confocal imaging on channel capillary slides mounted in a Zeiss LSM 880 inverted single photon point scanning confocal microscope equipped with a 32 GaAsP PMT channel spectral detector. Samples were imaged with a Zeiss Plan-Apochromat 63x 1.4 oil DIC objective, and excited at 488 nm by an Argon laser (1.75 mW) with a pinhole size of 0.57 and 1.05 airy units. Spectral scans were obtained from 410 to 695 nm with 8nm bandwidth. Using these settings, the background spectrum for each sample was obtained from dispersions of non-induced vesicles containing PURExpress and plasmid, and subsequently subtracted from the spectra recorded for vesicles containing the gene expression components and plasmid. For each experiment, multi-channel bright field and fluorescence images were obtained. All experiments

were maintained at 25°C using an incubation chamber. In general, the vesicles remained stable for over 24 hours.

Glucose-based signaling from lipid vesicles: Signaling between lipid vesicles and a GOx/HRP enzyme cascade in bulk solution at 37°C was undertaken as follows. Lipid vesicles containing PURExpress (25 µL), plasmid DNA - pET21b/*esaO*/α-hemolysin for α-hemolysin expression (1000 ng; DC055a), and glucose (137 mM) glucose were prepared as described above, and incubated with a solution (25 µL) containing GOx (50U/mL), HRP (5U/mL) and Amplex red (100 µM) with (10 µM) or without (HEPES buffer) 3OC6HSL. Production of resorufin was monitored over time by fluorescence spectroscopy (λ_{exc} = 570 nm, λ_{emi} = 575-700 nm). Errors were obtained by assuming a Gaussian distribution to the error i.e. standard deviation. Therefore the negative error is an artefact of the error analysis and not attributed to a negative fluorescence reading.

Lipid vesicle to proteinosome chemical signalling cascade: Lipid vesicles (1:2 POPC: cholesterol; 24.5 mM; pH = 7.6)) consisting of an encapsulated cell-free gene expression system (prepared as above), an encapsulated DNA plasmid (0.5-2 µg) with a T7 promoter, *esaO* operator, and insert coding for EsaR and either α-hemolysin (DC055a) and entrapped glucose (125 mM) were incubated at 37°C in an aqueous buffered (HEPES; pH = 7.6; (25 µL) dispersion of cross-linked HRP-containing GOx/PNIPAAM proteinosomes to produce a binary population of protocells. The number of vesicles were kept constant by calibrating the dispersions prior to addition of the proteinosomes by performing serial dilutions until a constant OD value of 0.2-0.3 was attained for absorbance measurements at 500 nm. Amplex red (HRP-substrate; 100 µM) and either 3OC6HSL (transcription inducer; 10 µM) or the equivalent volume of HEPES were then added to the external solution. The onset and rate of the fluorescent output (resorufin) arising from transmission of the glucose signal from the vesicles and activation of the enzyme cascade within the proteinosomes were monitored by fluorescence microscopy imaging and spectroscopy. Kinetic assays were undertaken on a Clariostar monochromator well plate reader (BMG; λ_{exc} = 550 +/- 20 nm , λ_{emi} = 590 +/- 10 nm). Aliquots obtained from the same batch of mixed vesicles and proteinosomes were loaded on ice into the well plate under sterile conditions, and then Amplex red and 3OC6HSL (or HEPES) added to each well. The well plate was covered and placed into the well plate reader at 37°C; each well was measured consecutively, with measurements recorded every 30 mins for 15 hours. At least four repeats were undertaken for experiments with or without the inducer molecule.

Supporting information:

Extended materials and methods; table of primers; fluoresence spectra of Cell free gene expression of EsaR-switchable RFP; results showing the determination of vesicles displaying GFP-tagged α-hemolysin expression; data for determination of diffusion coefficients; data for calcein leakage assay; data for intravesicular expression of α-hemolysin leading to glucose signalling to native GOx/HRP enzyme cascade; control GOx/HRP native enzyme assays; raw data for chemical communication between lipid vesicles and proteinosomes; residual data for kinetic fitting.

Author information:

***Corresponding author** S.mann@bristol.ac.uk ORCID:

tang@mpi-cbg.de ORCID: 0000-0001-9030-6991

Author contributions

SM and SSM conceived the project; SM, AWP, JLLRA, DC, AC and TYDT conceived and discussed the experiments; TYDT, DCC, GF, DA performed the experiments; TYDT, DCC, GF undertook the data analysis; SM and TYDT wrote the manuscript.

Notes

The authors declare no conflict of interest

Acknowledgements

We thank Richard Booth and Xin Huang for synthesis of mercaptothiazoline-activated PNIPAAm by Raft polymerization and Benoit Lombardot (Bioimage Informatics at MPI-CBG) for guidance with image analysis. We thank the Light Microscopy Facility at MPI-CBG, BBSRC/EPSRC-funded BrisSynBio Research Centre(BB/L01386X/1) for the use of well plate readers. The authors were supported by grants from the BrisSynBio (a BBSRC/EPSRC synthetic Biology research centre) (TYDT, AC, AWP, JLRA, SM); the MaxSynBio consortium (TYDT) (jointly funded by the Federal Ministry of Education and Research of Germany and the Max Planck Society) and MPG (DA); Erasmus (GF); Armenise-Harvard Foundation and the Simons Foundation (290358) (S. Mansy and DC) and a EPSRC Early Career Fellowship EP/K026720/1 (AWP).

References:

(1) Nourian, Z. and Danelon, C. (2013) Linking genotype and phenotype in protein synthesizing liposomes with external supply of resources. *ACS Synth. Biol. 2*, 186-193

(2) Martini, L. and Mansy, S. S. (2011) Cell-like systems with riboswitch controlled gene expression. *Chem. Commun. 47*, 10734-10736

(3) Huang, X., Li, M., Green, D.C., Williams, D.S.,Patil, A. J., and Mann, S. (2013) Interfacial assembly of protein-polymer nano-conjugates into stimulus-responsive biomimetic protocells. *Nature Commun. 4*, 2239.

(4) Huang, X., Patil, A. J., Li, M., and Mann, S. (2014) Design and Construction of Higher-order Structure and Function in Proteinosome-based Protocells *J. Am. Chem. Soc. 136*, 9225-9234

(5) Peters, R. J., Marguet, M., Marais, S., Fraaije, M.W., van Hest, J.C.M., and Lecommandoux, S. (2014) Cascade reactions in multicompartmentalized polymersomes. *Angew. Chem. Int. Ed. 53*, 146-150.

(6) Peters, R. J. R. W., Louzao, I. and van Hest, J. C. M. (2012) From polymeric nanoreactors to artificial organelles. *Chem. Sci. 3*, 335-342

(7) Li, M., Harbron, R. L., Weaver, J. V. M., Binks, B. P. and Mann, S. (2013) Electrostatically gated membrane permeability in inorganic protocells. *Nature Chem. 5*, 529-536.

(8) Torre, P., Keating, C. D. and Mansy, S. S. (2014) Aqueous multi-phase systems within water-in-oil emulsion droplets for the construction of genetically encoded cellular mimics. *Langmuir*, *30*, 5695-5699.

(9) Tawfik, D.S. and Griffiths, A.D. (1998) Man-made cell-like compartments for molecular evolution. *Nature Biotechn. 16*, 652-656.

(10) Koga, S., Williams, D. S., Perriman, A. W. and Mann, S. (2011) Peptide-nucleotide microdroplets as a step towards a membrane-free protocell model. *Nature Chem. 3*, 720-724

(11) Huang, X., Li, M., and Mann, S. (2014) Membrane-mediated Cascade Reactions in Enzyme-polymer Proteinosomes *Chem. Commun. 50*, 6278-6280

(12) Holden, M. A., Needham D, and Bayley, H. (2007) Functional bionetworks from nanoliter water droplets. *J. Am. Chem. Soc. 129*, 8650-8655.

(13) Nomura, S. I. M., Tsumoto, K., Hamada, T., Akiyoshi, K., Nakatani, Y., and Yoshikawa, K. (2003) Gene expression within cell-sized lipid vesicles. *ChemBioChem*. *4* , 1172-1175.

(14) Noireaux, V., Bar-Ziv, R., Godefroy, J., Salman, H., and Libchaber, A., (2005) Toward an artificial cell based on gene expression in vesicles *Physical biology. 2*, no. 3: P1

(15) Tang, T-Y D., van Swaay, D., deMello, A., Anderson, J. L R., and Mann, S. (2015) *In vitro* gene expression within membrane-free coacervate protocells. *Chem. Commun. 51*, 11429-11432.

(16) Li, M., Green, D. C., Anderson, J.L.R, Binks, B. P., and Mann, S. (2011) *In vitro* gene expression and enzyme catalysis in bio-inorganic protocells. *Chemical Science. 9*, 1739-1745.

(17) Kita, H., Matsuura, T., Sunami, T., Hosoda, K., Ichihashi, N., Tsukada, K., Urabe, I. and Yomo, T. (2008) Replication of genetic information with self-encoded replicase in liposomes. *ChemBioChem*. *9*, 2403-2410,.

(18) Chen, I.A., Salehi-Ashtiani, K. and Szostak, J.W. (2005) RNA catalysis in model protocell vesicles. *J. Am. Chem. Soc. 127,* 13213-13219.
(19) Weitz, M., Kim, J., Kaspner, K., Winfree, E., Franco, E. and Simmel, F.C., (2014) Diversity in the dynamical behaviour of a compartmentalized programmable biochemical oscillator, *Nature Chem. 6*, 295–302
(20) Zhu, T.F. and Szostak, J.W. (2009) Coupled growth and division of model protocell membranes. *Journal of the American Chemical Society*, *131*, 5705-5713.
(21) Wen, P., Liu, X., Wang, L., Li, M., Huang, Y., Huang, X., and Mann S. (2017) Coordinated Membrane Fusion of Proteinosomes by Contact-Induced Hydrogel Self-Healing. *Small 13* doi: 10.1002/smll.201700467.
(22) Noireaux, V., Bar-Ziv, R. and Libchaber, A. (2003) Principles of cell-free genetic circuit assembly. *Proceedings of the National Academy of Sciences*. *100*,12672-12677.
(23) Siegal-Gaskins, D., Tuza, Z.A., Kim, J., Noireaux, V. and Murray, R.M. (2014) Gene circuit performance characterization and resource usage in a cell-free "breadboard". *ACS synthetic biology*. *3*, 416-425
(24) Nakano, T., Moore, M., Enomoto, A., and Suda, T. (2011) Molecular Communication Technology as a Biological ICT. *Biological Functions for Information and communication Technologies, Studies in Computational Intelligence*, *320,* DOi: 10.1007/978-3-642-15102-2_2, Springer-Verlag Berlin Heidelberg, 49-85
(25) Stano, P., Rampioni, G., Carrara, P., Damiano, L.,Leoni, L., and Luigi Luisi, P. (2012)Semi-Synthetic minimal cells as a tool for biochemical ICT. *Biosystems*. *109*, 24-34
(26) Gardner P. M., Winzer, K. and Davis, B. G. (2009) Sugar synthesis in a protocellular model leads to a cell signalling response in bacteria. *Nature Chem. 1*, 377-383.
(27) Lentini, R., Santero, S.P., Chizzolini, F. and Mansey, S.S. (2014) Integrating artificial with natural cells to translate chemical messages that direct E. coli behaviour. *Nature Commun. 5*, 4012.
(28) Lentini, R., Martín, N.Y., Forlin, M., Belmonte, L., Fontana, J., Cornella, M., Martini, L., Tamburini, S., Bentley, W.E., Jousson, O. and Mansy, S.S. (2017) Two-way chemical communication between artificial and natural cells. *ACS central science*. *3*, 117-123.
(29) Schwarz-Schilling, M., Aufinger, L., Muckl, A and Simmel, F. C. (2016) Chemical communication between bacteria and cell-free gene expression systems within linear chains of emulsion droplets. *Integrative Biology. 8*, 564-570
(30) Qiao, Y., Li, M., Booth, R., and Mann S. (2017) Predatory Behaviour in Synthetic Protocell Communities *Nature Chemistry. 9*, 110-119
(31) Rodríguez-Arco, L., Li M., and Mann S., (2017) Phagocytosis-inspired Behaviour in Synthetic Protocell Communities of Compartmentalized Colloidal Objects. *Nature Materials 16*, 857-863
(32) Sun, S., Li, M., Dong, F., Wang, S., Tian, L., and Mann, S. (2016) Chemical Signaling and Functional Activation in Colloidosome-Based Protocells. *Small*. 12, 1920–1927
(33) Adamala, K.P., Martin-Alarcon, D.A., Guthrie-Honea, K.R. and Boyden, E.S. (2017)Engineering genetic circuit interactions within and between synthetic minimal cells. *Nature chemistry*. *9*, 431.
(34) Gambin, Y., Lopez-Esparza, R., Reffay,M., Sierecki, E., Gov, N.S., Genest, M.H.R.S., Hodges, R.S. and Urbach, W. (2006) Lateral mobility of proteins in liquid membranes revisited. *Proceedings of the National Academy of Sciences of the United States of America*. *103*, 2098-2102.
(35) Kumar, M., Mommer, M.S. and Sourjik, V. (2010) Mobility of cytoplasmic, membrane, and DNA-binding proteins in Escherichia coli. *Biophysical Journal*. *98*, 552-559
(36) Andersson, A., Danielsson, J., Gräslund, A. and Mäler, L. (2007) Kinetic models for peptide-induced leakage from vesicles and cells. *European Biophysics Journal*. *36*, 621-635
(37) Vogt, T.C. and Bechinger, B. (1999) The Interactions of Histidine-containing Amphipathic Helical Peptide Antibiotics with Lipid Bilayers; the effects of charges and pH. *Journal of Biological Chemistry*. *274*, 29115-29121.
(38) de Souza, T.P., Fahr, A., Luisi, P.L. and Stano, P. (2014) Spontaneous encapsulation and concentration of biological macromolecules in liposomes: an intriguing phenomenon and its relevance in origins of life. *Journal of molecular evolution*. *79*, 179-192.
(39) Barkai, N. and Shilo, B.Z. (2007) Variability and robustness in biomolecular systems. *Molecular cell*. *28*, 755-760.
(40) Eldar, A. and Elowitz, M.B. (2010) Functional roles for noise in genetic circuits. *Nature*. *467*, 167.
(41) Herranz, H. and Cohen, S.M. (2010) MicroRNAs and gene regulatory networks: managing the impact of noise in biological systems. *Genes & development*. *24*,1339-1344.
(42) Samoilov, M.S., Price, G. and Arkin, A.P. (2006) From fluctuations to phenotypes: the physiology of noise. *Sci. STKE*. *366*, re17-re17.
(43) Adamala, K., Engelhart, A.E., Kamat, N.P., Jin, L. and Szostak, J.W. (2015) Construction of a liposome dialyzer for the preparation of high-value, small-volume liposome formulations. *Nature protocols*. *10*, 927-938.

Figures:

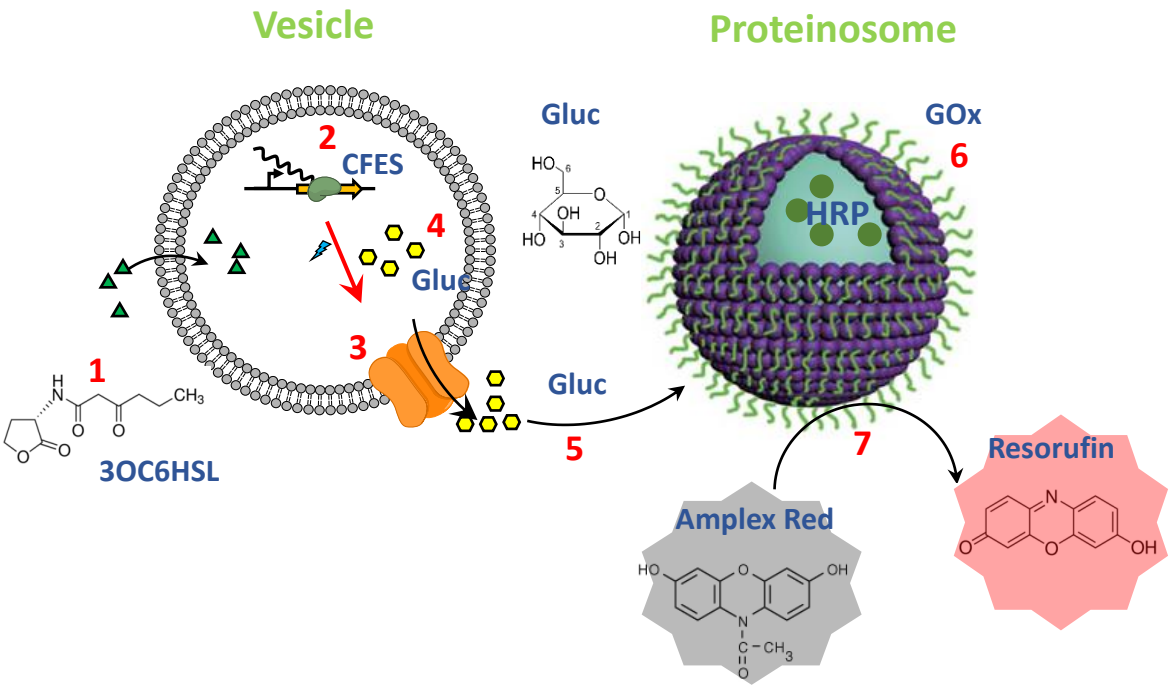

Figure 1: Schematic showing general strategy for gene-directed chemical communication from lipid vesicles to proteinosomes in a binary population of synthetic protocells. Lipid vesicles containing a DNA plasmid, cell-free gene expression system (CFES) and a small molecule signalling molecule (glucose; Gluc; yellow hexagons) were prepared from a 1:2 molar ratio of POPC and cholesterol. The plasmids consisted of a T7 promoter, *esaO* operator, an insert code for an *esaO* -binding repressor protein (EsaR) that was responsive to N-(3-Oxohexanoyl)-L-homoserine lactone (3OC6HSL) (transcription inducer); and a gene for a membrane porin (α-hemolysin (DC055a) or GFP-tagged α-hemolysin (DC061a)). Proteinosomes consisting of a semi-permeable membrane of crosslinked glucose oxidase (GOx)-PNIPAAm nanoconjugates (green/purple objects) and encapsulated horseradish peroxide (HRP; green circles) were prepared as previously reported [12] and dispersed in HEPES buffer. Chemical communication from the transmitting protocells (vesicles) to the receivers (proteinosomes) was achieved using a bottom-up modular approach comprising transcriptional induction by 3OC6HSL influx (**1**), cell-free gene expression of α-hemolysin (**2**), membrane insertion of α-hemolysin (**3**), porin-induced efflux of glucose (**4**), diffusion-mediated glucose signaling of an enzyme cascade (**5**), oxidation of glucose on the GOx-PNIPAAm proteinosome membrane to produce D-glucono-δ-lactone and hydrogen peroxide (**6**), HRP-mediated peroxidation of Amplex red within the proteinosomes to generate a red fluorescent read-out (resorufin) (**7**).

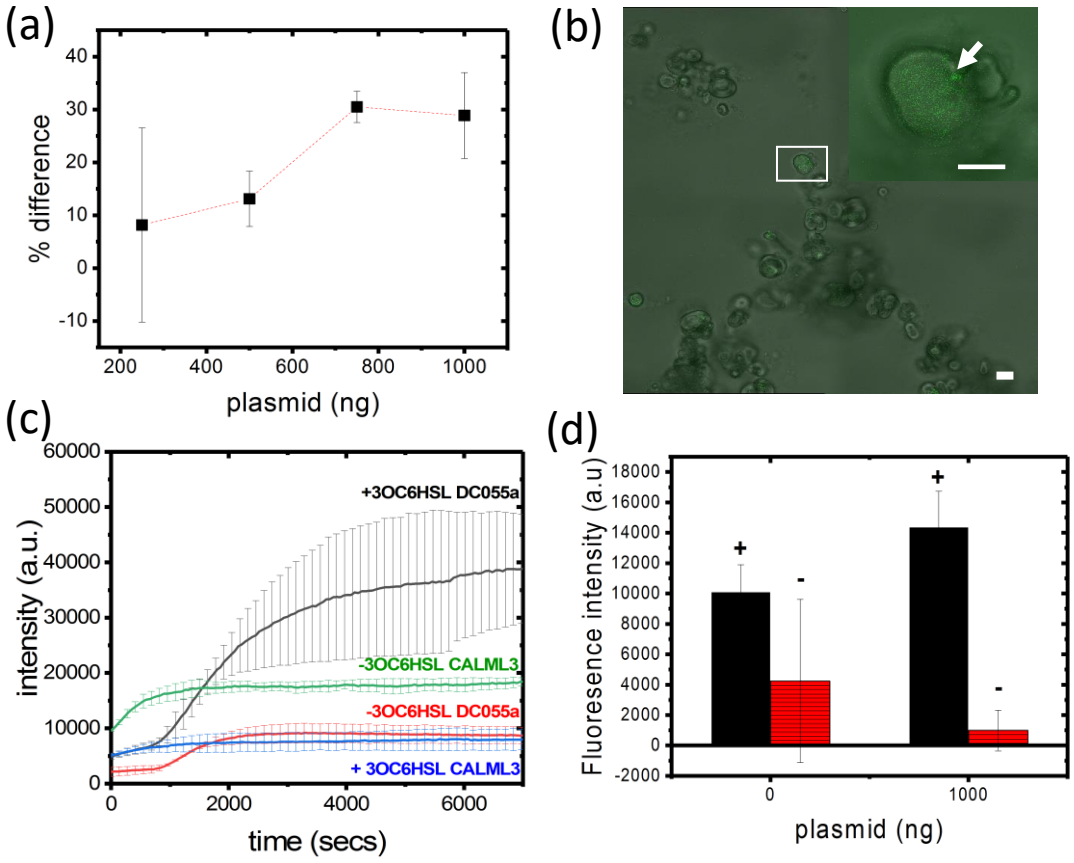

Figure 2: Modular design of lipid vesicles for cell-free gene-directed chemical communication. **(a)** *Testing of the EsaR switch*: Plot showing changes in the percentage difference between the fluorescence peak maxima of induced and non-induced RFP expression measured at a constant plasmid concentration, and repeated over a range of plasmid concentrations. Varying concentrations of a pET21b/*esaO*/RFP plasmid construct (DC054a) for RFP expression were mixed with a cell-free gene expression system (PURExpress) and incubated at 37°C with or without 10 μM of the transcription inducer 3OC6HSL (total volume, 14 μL), and fluorescence spectra, (λ_{exc} = 563 nm, λ_{emi} = 582-700 nm) recorded. **(b)** *GFP-tagged α-hemolysin expression in lipid vesicles*: Fluorescence confocal microscopy image of vesicles undergoing spatially confined gene-mediated protein synthesis showing regions of localized green fluorescence close to the inner leaflet of the membrane and within the vesicle. Inset shows high magnification image of delineated area (white box) showing localized fluorescence intensity associated with the vesicle membrane (white arrow) and lumen. The image is processed to reveal levels of GFP fluorescence above the average background level recorded from spectral scans of vesicles not exposed to the transcription inducer 3OC6HSL. The vesicles (1:2 POPC:cholesterol; final concentration, 24.5 mM) were prepared using an aqueous mixture (25 μL) containing 2 μg of a pET21b/*esaO*/α-hemolysin-GFP plasmid construct (DC061a) for GFP-tagged α-hemolysin expression. Non-encapsulated components were removed by dialysis, and the vesicles incubated with 10 μM 3OC6CHSL or an equivalent aqueous volume of HEPES buffer at 37°C for at least 3 hours. Scale bars = 10 μm (inset = 5 μm). **(c)** *Expression of α-hemolysin leads to small molecule release from the vesicles*. Plot showing time-dependent increase in fluorescence intensity at 37°C for calcein-containing vesicles incubated in a bulk aqueous solution (pH 7.6; 25 μL) containing PURExpress and a pET21b/*esaO*/α-hemolysin DNA plasmid construct encoding for α-hemolysin (DC055a; 1000 ng) with (black, 10 μM) or without (red, HEPES buffer) the 3OC6HSL transcription inducer. Initially, self-quenching of calcein (80 mM) produced low fluorescence intensities, which increase with time particularly in the presence of 3OC6HSL showing an

approximately of 350% increase in calcein fluorescence with 3OC6HSL versus without after 1 hr and 50 mins. The increase in fluorescence was associated with a decrease in the intravesicular dye concentration, and consistent with expression and membrane assembly of the porin, and sustained calcein release. Experiments in which the DC055a plasmid was replaced with a PEXP-NT/CALML3 plasmid encoding for the non-porin protein, calmodulin in the presence (blue) and absence (green) of 3OC6HSL showed only minimal leakage of calcein from the vesicles. **(d)** *Glucose release from vesicles initiates the onset of an enzyme cascade.* Plot showing averaged peak maxima fluorescence intensities (λ_{exc} = 570 nm, λ_{emi} = 575-700 nm) recorded for resorufin production after 3 h (end point data) in reaction mixtures consisting of GOx (50 U/mL), HRP (5 U/mL) and Amplex red (100 μM), and a dispersion of vesicles containing PURExpress (25 μL), a pET21b/*esaO*/α-hemolysin DNA encoding for α-hemolysin (1000 ng; (DC055a)), and glucose (137 mM). Experiments were undertaken in the presence (black, 10 μM) or absence (red; HPES buffer) of the 3OC6HSL transcription inducer, which was added to the external solution. A marked increase in enzyme cascade activity was observed in the gene-mediated system in the presence of 3OC6HSL in contrast to without the inducer. Resorufin production was also observed but at a reduced level in control experiments undertaken in the absence of the plasmid.

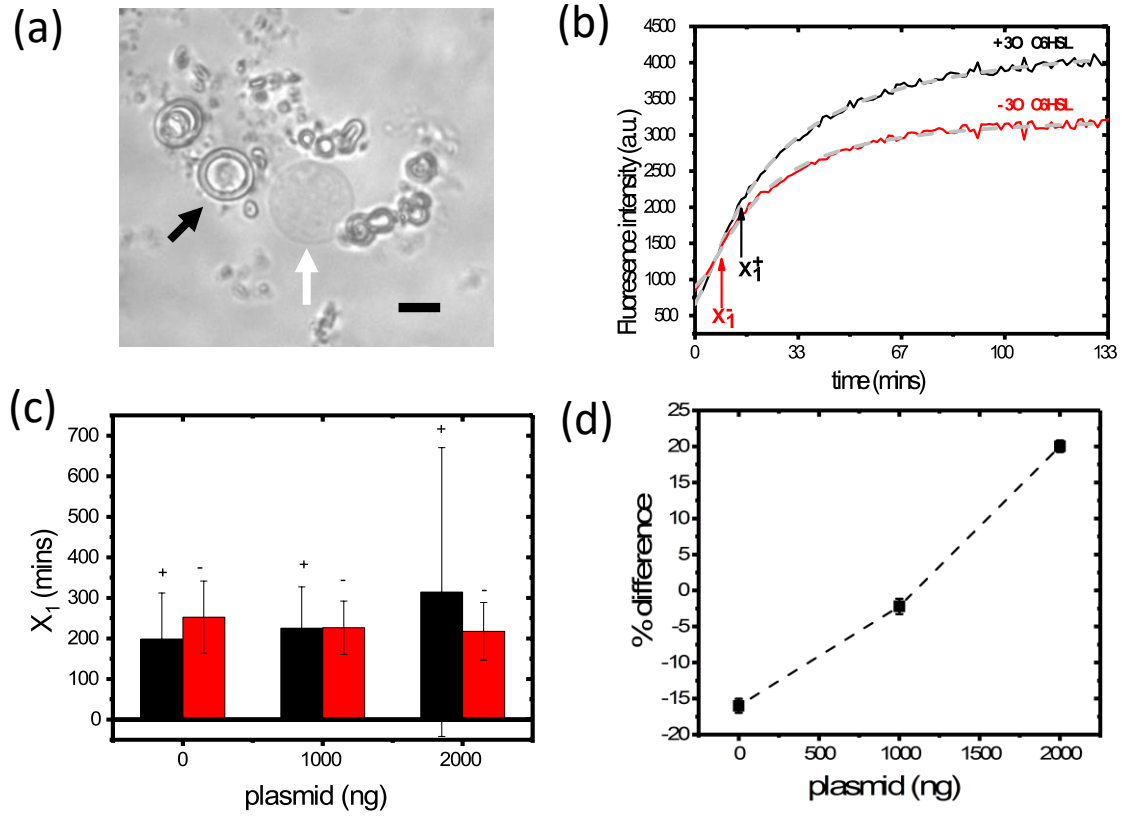

Figure 3: Chemical communication from vesicles to proteinosomes. (a) Bright field optical microscopy image showing a binary population of HRP-containing GOx/PNIPAAm proteinosomes (white arrow) and vesicles containing encapsulated PURExpress, glucose, and a pET21b/*esaO*/α-hemolysin (DC055a) encoded for α-hemolysin expression (black arrow). The proteinosomes were 20-40 µm in average size, and typically larger than the vesicles. Scale bars = 10 µm. (**b**) Plots showing increases in fluorescence intensity with time associated with resorufin production generated by gene-mediated transmission and delivery of glucose from vesicles to enzymatically active proteinosomes in the presence (black) and absence (red) of the transcription inducer 3OC6HSL. Vesicles were prepared in the presence of 2000 ng plasmid. The kinetic plots were fitted to a logistic model (grey) and the stationary points for induced (X_1^+) and non-induced (X_1^-) communication obtained to obtain a semi-quantitative comparison between each of the data sets recorded. Stationary points correspond to the time value on each curve where the second derivative is = 0. (**c,d**) Analysis of resorufin production from time course data. Plot showing stationary points (X_1) obtained for time-dependent resorufin fluorescence from a vesicle/proteinosome communication pathway in the presence (black) or absence (red) of 3OC6HSL at a range of plasmid concentrations (**c**). Error bars are from standard deviations of multiple aliquots (minimum four) obtained from the same batch of vesicles and proteinosomes, and are typically large. To reduce the error bars, the percentage difference between the stationary points for induced (X_1) and non-induced (X_1) communication systems were determined (averaged over at least 6 different vesicles/proteinosomes batches) and plotted against plasmid concentration (**d**). Increased plasmid levels were associated with a positive percentage difference, indicating that under these conditions the production of resorufin under the activity of 3OC6HSL was more sustained than without the transcription inducer.